International Journal of Innovative Technology and Exploring Engineering (IJITEE)
ISSN: 2278-3075 (Online), Volume-4 Issue-7, December 2014

An Interactive Design Tool for Engine Sand Separator System

Farooq Saeed

Abstract—This paper presents the details of development of an efficient interactive design tool for aircraft engine sand separator systems. The development of such a tool was felt necessary to address the problem of sand ingestion in gas turbine engines; a vital concern for the aviation and gas-turbine based electricity generation industry communities operating in desert environments as it can seriously affect the operation, performance and life cycle of a turbine engine. The design tool makes use of state-of-the-art practical geometry design and analysis technique, namely the inverse airfoil design method for the design of specific profiles for engine air intakes. The sand separator design is achieved by giving a specific contour to the intake profile, such as a highly curved bend in the duct, so that the contaminants because of their inertial momentum are forced away from the central flow. Since the sand particles can rebound of the air intake walls and enter the engine, the method takes into account sand particle rebound or restitution characteristics in the design. The design is accomplished with the aid of optimization techniques in both the inverse aerodynamic design as well as in the sand separator system design. In addition, to facilitate the analysis and design in an interactive manner, a MATLAB GUI has been developed. Details of the analysis and design tool are presented along with simple but practical design examples to demonstrate the usefulness and utility of the method and the interactive tool

Index Terms—Sand ingestion, inertial particle separator, inverse airfoil design, potential flow, sand particle trajectory

I. INTRODUCTION

Areas surrounding the Arabian Gulf region are known for their harsh desert-like environment where the air is usually laden with sand and dust particles. Aircrafts operating under such conditions for long periods are vulnerable to internal engine damage. The region also generates its electricity entirely from one of the largest fleet of gas turbine engines. Sand ingestion is, therefore, a vital concern for the regional aviation and power generation authorities. It is well known that the operational life of a turbine engine operating in sandy environments can be as short as 50 hours (Ref. 1, 2). Engine damage can range from simple erosion in the engine blades, to a completely inoperative engine with as little as half a pound of sand (Ref. 3). In addition, the degradation in performance and efficiency of the turbine engine leads to an increases in fuel consumption and operational cost (Ref. 1). Aramco Aviation, which provides major aerial transportation support services to Saudi Aramco, the biggest oil company in the world, operates both fixed and rotary-wing aircraft out of sand/desert strips in remote oil and gas fields spread all over the region. Aramco Aviation experience in operating from these remote areas has evidenced significant performance degradation and lifetime reduction of its aircraft turbine engines primarily due to sand erosion. Figures 1(a) and (b) provided by Aramco Aviation (Ref. 4) reveal the harmful effects of sand erosion on turbine vanes and blades, respectively. They attribute this damage to the presence of fine dust and sand together with high moisture content in the region. Aramco Aviation also had to prematurely remove all of the engines from its fleet of Dash-8 aircraft within the first year of its service (about 1,000 hours) due to damage caused by sand ingestion. In addition, aircraft air conditioning and filtration systems were also amongst the major areas affected by the sand particles which without adequate maintenance specific to the regional environment were found to survive only one-fifth of their expected life. In Fig. 1, a physical examination of the effects of sand erosion reveals blunted leading edges, sharpened trailing edges, reduced blade chords, and increased pressure surface roughness. Studies (Ref. 5, 6) have found erosion in turbo-machinery to be principally related to the gas flow path and sand particle size, and to a lesser degree to other factors such as the ingested sand particle characteristics, blade geometry, internal engine passages, environmental and operating conditions, and blade material. It, therefore, becomes imperative that some form of protective device, such as an Inertial Particle Separator (IPS) system, must be employed in the air intake of turbine engines operating in desert environment to prolong their operational life and to provide sustained performance. Thus, the use of an IPS system is a recommended practice in desert-like environments. Currently there are two types of IPS systems in use: the swirl and the vaneless type. In the swirl type, vanes introduce a swirl to the contaminated inlet flow. The resulting centrifugal force causes the heavier sand particles to move over to the outer periphery and into a scavenge duct. The vaneless type relies on the specific contour of the inner walls of the inlet and the diffuser that direct the contaminants to the scavenge duct. Figure 2 (Ref. 3), shows a sketch of a typical IPS system installed on the engine inlets of helicopters (such as Boeing CH-47D) which resembles an axisymmetric, bifurcated duct. Contaminated air enters the device through the inlet annulus on the left, and around a sharp bend, B. The bend is designed in such a manner that the inertia of the contaminants is sufficient to prevent them from following the air around the bend. Thus a significant portion of contaminants, such as sand, dust, etc., pass into a scavenge passage, A, and the almost contaminant-free clean air passes into the engine along the inner annulus. The IPS system does a phenomenal job of keeping the engines clean and free from damage due to sand particles and other foreign object ingestion.

Manuscript published on 30 December 2014.
***Correspondence Author(s)**
Prof. Farooq Saeed, Department of Aerospace Engineering, King Fahd University of Petroleum & Minerals, Dhahran, Saudi Arabia.

Inertial particle separator systems (such as that shown in Fig. 2) are capable of moving large particles leaving the smaller ones to be trapped by the filters which greatly enhanced the life of the filter and offers maximum engine protection. However, recent military operations in the Middle East have raised the problem of inefficiency of existing IPS system designs (Ref. 7) and suggest that the IPS system designs were not specifically tailored to the local or regional environmental conditions. A survey of existing design techniques for IPS system reveals that these design techniques are very costly since they make use of extensive direct analysis techniques along with experimental validation (Ref. 8–10) whereby the IPS system geometry is continuously improved via numerous iterations, i.e., through hit-and-trial.

Owing to the shortcomings of the current design techniques, the current study presents a novel and more efficient design tool as well as a method for the design of an IPS system in that the design is accomplished in a single step not via direct geometry specification but through specification of the design requirements (engine mass flow rate, flight conditions, etc.) and constraints on the geometry (gas flow path, sand particle size, nacelle size, etc.) in an inverse fashion as opposed to the direct hit-and-trial technique. Moreover, to facilitate the design, a MATLAB GUI tool has been developed. A partial implementation of this idea has also resulted in a US Patent No. 7922784 (Ref. 11) and related publications (Ref. 12 & 13).

A recent study (Ref. 14) has shown that solid particle erosion in turbines can be reduced by using suitable nozzle passage design to control the particle impacting velocity and impacting angle. In an inverse geometry design (Ref. 15–18) particle impact characteristics can be used as a constraint on the design resulting in a geometry that is safe from erosion. Another important and unique advantage and strength of the inverse design technique is in its multi-point design capability in which multiple design requirements can be met simultaneously and, hence, the designed geometry performs equally well under "on- or off-design" conditions. Furthermore, the design method fully incorporates sand particle rebound characteristics derived from experiments in the design making it a very reliable tool for trade-off and practical design studies.

In the sections that follow, a brief description of the IPS analysis and design tool and its various functions is presented along with the design methodology and its implementation. The paper then presents a few design examples to illustrate the utility and strengths of the tool. Finally, the paper ends with some main conclusions

II. IPS DESIGN AND ANALYSIS TOOL

This section presents the details of the IPS analysis and design tool and the design methodology developed in this investigation. Figure 3 represents an example of a typical IPS system, modeled after a typical axisymmetric helicopter engine particle separator shown in Fig. 2, represented as a five-element airfoil configuration. The individual airfoil elements are numbered 1 through 5 such that they represent the central hub (element 1), the engine housing (elements 2 & 3), and the outer engine cowling (elements 4 & 5). Taking advantage of symmetry about the engine centerline, only elements 1, 2 and 4 need to be designed since elements 3 and 5 are mirror images of elements 2 and 4, respectively. A careful examination of Fig. 3 suggests that the path of sand particles can be controlled by an appropriate channeling of their flow paths which can be achieved by giving a specific contour to the surface areas where the particles impact as well as positioning of airfoil elements 1 through 5. Since particle paths are to a great degree influenced by the rebound characteristics, these characteristics could be used to determine the appropriate surface curvature. Thus, the new design method makes use of both the particle inertia as well as rebound characteristics as a means to direct particle paths towards scavenge areas. Since particle flow path as well as rebound characteristics depend on the IPS system geometry, the inverse airfoil design methodology (Ref. 15–18) is employed to obtain the desired geometry through specification of the required flow and rebound characteristics.

To facilitate analysis and design, a MATLAB GUI (Graphical User Interface) was developed to carryout analysis or design in an interactive manner. The GUI, shown in Fig. 4, performs four major tasks or functions, namely: (1) Initialization, (2) Analysis, (3) Inverse design, and (4) Optimization. Details of these functions are as follows:

A. Initialization Function

The initialization function defines an initial configuration of a multi-element airfoil based IPS system. This is achieved by generating multiple airfoil geometries and positioning them subject to a set of geometric constraints such as size of the engine and inlet in terms of maximum diameter and length of each airfoil element. The first step in this process is to design individual airfoil geometries that will represent the central hub (element 1), the engine housing (elements 2 & 3), and the outer engine cowling (elements 4 & 5). The design of these individual airfoils is accomplished with the help of PROFOIL, the multipoint inverse airfoil design code (Ref. 15–18). The inverse design methodology implemented in PROFOIL is presented later in this paper. The GUI is used to define initial airfoil geometries and load them into the design space, each airfoil element at a time, by altering the PROFOIL input script to generate the IPS airfoil elements. The GUI can also be used to interactively scale, rotate or position individual airfoil geometries to generate the multi-element IPS configuration. A user-defined design box function is also provided to restrict the elements inside the box, were the width and height of the box can be specified by the designer.

B. Analysis Function

Once the geometry has been defined, the second step is the flow and trajectory analysis of a multi-element airfoil configuration. The flow analysis function employs the panel method of Hess and Smith (Ref. 19) which is an inviscid flow analysis method that has been modified for analysis of for multi-element airfoil configurations. This method determines the velocity potential field around multi-element airfoil configurations which is used to simulate particle trajectories through the IPS system.

Published By:
Blue Eyes Intelligence Engineering
and Sciences Publication (BEIESP)

To determine the sand particle trajectory, a force/momentum balance is applied on a particle moving through air. Similar studies related to sand and water droplet impingement and ice accretion on aircraft and engine inlet surfaces are available in literature (Ref. 20–23). The same approach has been used in this study. The resulting momentum equation in 2D is:

$$\frac{d^2\vec{r_p}}{dt^2}+\frac{C_d\,\mathrm{Re}}{24K_a}\frac{d\vec{r_p}}{dt}=K_g(\sin\theta\vec{i}-\cos\theta\vec{j})+\frac{C_d\,\mathrm{Re}}{24K_a}\vec{V_a} \qquad (1)$$

In the above equation, K_g and K_a are the non-dimensional particle bouyancy and inertia paramemters, respectively, while Re is the Reynolds number based on droplet equivolumetric diameter D_{eq}, and C_d is the particle drag coefficient. These parameters are defined as:

$$K_g=\frac{(\rho_p-\rho_a)g}{\rho_p};K_a=\frac{\rho_p D_{eq}^2}{18\mu_a};\mathrm{Re}=\frac{\rho_p D_{eq}U}{\mu_a} \qquad (2)$$

Where $\vec{r_p}$ and $\vec{V_p}$ represent particle position and velocity vectors with respect to the particle-fixed reference frame, $\vec{V_a}=u_a\vec{i}+v_a\vec{j}$ is the free stream velocity, $\vec{U}=\vec{V_a}-\vec{V_p}$, is the particle relative velocity, ρ_p and ρ_a are the particle and air densities, μ_a is the viscosity of air, and g is the gravitational acceleration.

Equation (1) is a second-order non-linear differential equation because of the term $C_d\,\mathrm{Re}/(24K_a)$, which depends on the particle position and velocity. The difficulty to determine the term $C_d\,\mathrm{Re}/(24K_a)$ suggests that a numerical technique must be employed to integrate the momentum equation. The well-known fourth-order Runge-Kutta method (Ref. 24) is used to integrate the momentum equation. The particle trajectories are initiated at a distance of about five chord lengths (of the middle airfoil representing the engine centerline) and are calculated by numerically integrating Eq. (1) until the particle crosses a pre-selected location along the axial direction, typically past the entrance to the engine core flow which in the present investigation is fixed at the trailing edge location of the outer elements 4 and 5. Greater details of the method can be found in Ref. 20.

The particle, as it moves through the IPS system may or may not impact the different elements. The particle collision with the surface could be treated as elastic or inelastic, however, inelastic collisions have been found to give more accurate scavenge efficiencies. In literature (Ref. 25–28), the inelastic impacts are characterized by restitution coefficients that are ratios relating the incident and rebound angles (β_1, β_2) and velocities (V_1, V_2) and its components before and after the impact (see Fig. 5). These restitution coefficients are obtained from experiments and are expressed as fourth-degree polynomials that are a function of the particle incident angle β_1. In the present investigation, the restitution coefficients reported by Tabakoff and Hamed (Ref. 29) for their aluminum target surface have been used and are given by:

$$\begin{aligned}
\frac{V_2}{V_1}&=1-2.03\beta_1+3.32\beta_1^2-2.24\beta_1^3+0.472\beta_1^4\\
\frac{\beta_2}{\beta_1}&=1+0.409\beta_1-2.52\beta_1^2+2.19\beta_1^3-0.531\beta_1^4 \qquad (3)\\
\frac{V_{n2}}{V_{n1}}&=0.993-1.76\beta_1+1.56\beta_1^2-0.49\beta_1^3\\
\frac{V_{t2}}{V_{t1}}&=0.988-1.66\beta_1+2.11\beta_1^2-0.67\beta_1^3
\end{aligned}$$

The new particle location is determined after impact and rebound from where once again the particle momentum equation is used to track particle after impact. This step is repeated after each impact till the particle crosses the trailing edge location of the outer elements 4 and 5. The entire trajectory, impact and rebound procedure is repeated for each sand particle released in the flow from different upstream locations (y_0) along the y-axis while keeping a constant upstream distance of five chord lengths ($x_0 = -5c$).

Another important requirement for an efficient design of an IPS system is the knowledge of sand particle characteristics which may be specific to the region. Sand in nature is composed of fine rock and mineral particles that have been altered by chemical and environmental conditions, and affected by processes such as weathering or erosion. With all the diversity in soil, sand grains are typically made up of silica or its polymorphs such as quartz. In geology, sand is categorized as a soil grain with a predefined particle size and range without consideration of the type of grain material. Many soil grain size distribution standards exist in geology and engineering. Typically, sand grain is classified as fine sand in the 0.06 – 0.425 mm (60 – 425 microns) range, medium between 0.425 – 2.0 mm and coarse between 2.0 – 4.75 mm. Figure 6 is a map of soil grain sizes in the Middle East (Ref. 7).

The knowledge of sand gain size and shape are important since they are directly related to the lift and drag of the sand particles. Studies indicate that there is no lift if the particle does not have a rotational movement and keeps an axisymmetric shape relative to the flow, and if the flow is irrotational. On the basis of this assumption, the lift force can be treated as zero and thus only the drag force needs to be considered. Moreover, because the small size of the particles is in the range where shear forces cannot be neglected, the drag force evaluation needs to consider both pressure and shear forces. Since, such a calculation can be very demanding, a more convenient and commonly used method in studies related to sand particles is to use some form of empirical correlation for the drag coefficient of particle. In the sphere drag measurement experiments, the terminal velocity of falling spheres in stagnant medium (air or fluid) was measured. For this terminal velocity, the drag force is equal to the weight force less the buoyancy force. With this data, it is easy to determine the drag coefficient C_d for various Reynolds numbers. Figure 7 shows a comparison of sphere drag coefficient empirical correlations proposed by various authors (Ref. 30–38). As evident from the figure, all of the correlations agree upto a Re = 1000.

Brown and Lawler (Ref. 38) recently re-evaluated the experimental sphere drag data available in literature to account for the effect of walls since much of the data was measured in small diameter cylindrical vessels. They proposed new correlations for the drag coefficient based on corrected experimental data. In the current project, the new sphere drag coefficient correlation based on Eq. (19) of Ref. 38 has been considered since it provides the best fit to the existing experimental data for the entire range of Reynolds number ($10^{-3} \leq \mathrm{Re} \leq 3.5\times10^5$) considered . The correlation is given by the relation:

Published By:
Blue Eyes Intelligence Engineering
and Sciences Publication (BEIESP)

$$C_d = \frac{24}{\mathrm{Re}}\left(1+0.150\,\mathrm{Re}^{0.681}\right)+\frac{0.407}{1+\frac{8710}{\mathrm{Re}}} \quad (4)$$

Since sand particles are non-spherical, drag coefficient correlations for non-spherical particles were also compared for error and range of applicability. Chhabra et al. (Ref. 25) have critically evaluated the widely-used drag correlations from 19 studies with a resulting data base of 1900 data points for a range of Reynolds number ($10^{-4} \le \mathrm{Re} \le 5\times10^5$). One of the methods investigated by Chhabra et al. was the Haider and Levenspiel's non-spherical correlation (Ref. 35); valid for the particle Reynolds number less than 2.5×10^5. The maximum particle Reynolds number observed in this study (for very fine to coarse size particles and a velocity of 40 m/s) was of the order of 100 to 1500, respectively. Haider and Levenspiel relate the shape of a non-spherical particle by a shape factor ϕ which is defined as the ratio of the surface area of a sphere having the same volume as the particle to the actual surface area of the particle. Thus for non-spherical particles: $0 < \phi < 1$. The sand particle shape factor can vary from 0.3 to as high as 0.9. The drag coefficient correlation of Haider and Levenspiel (Ref. 35) for non-spherical particles with a shape factor ϕ is given by:

$$C_d = \frac{24}{\mathrm{Re}}\left(1+b_1\,\mathrm{Re}^{b_2}\right)+\frac{b_3+\mathrm{Re}}{b_4+\mathrm{Re}} \quad (5)$$

where

$$b_1 = \exp(2.3288 - 6.4581\phi + 2.4486\phi^2)$$
$$b_2 = 0.0964 + 1.5565\phi$$
$$b_3 = \exp(4.905 - 13.8944\phi + 18.4222\phi^2 - 10.2599\phi^3)$$
$$b_4 = \exp(1.4681 + 12.258\phi - 20.7322\phi^2 + 15.8855\phi^3)$$

The results of Chhabra et al. (Ref. 25) indicate that Haider and Levenspiel correlation satisfactorily predicts drag for particle with values of $\phi > 0.67$. Figure 8 shows a comparison of the Haider and Levenspiel correlation (for non-spherical particles) prediction with other methods. It is evident from the figure that for small values of shape factor (elongated shape), a significant increase in drag results, e.g. for $\phi < 0.5$, the non-spherical particle drag can be as high as 6-7 times. In the current study, a shape factor of $\phi = 1$ has been considered along with the drag coefficient correlation of Brown and Lawler, Eq. (5) above. In addition, a sand particle density ρ_p = 1422 kg/m^3 has been used.

C. Inverse Design Function

The inverse design function is used for interactive design of the individual airfoil geometries once the particle trajectory and impact characteristics have been determined. The inverse airfoil design approach is an attractive alternative to the existing IPS system design methods employing the direct design approach through hit-and-trial (Fig. 9). In an inverse design method, the design is accomplished in a single step not via direct geometry specification but through specification of the design requirements such as lift or geometrical constraints, or desired velocity distribution(s) (Fig. 9) subject to certain constraints. A recent study (Ref. 14) has shown that solid particle erosion in turbines can be reduced by using suitable nozzle passage design to control the particle impacting velocity and impacting angle. Thus, in an inverse design, geometrical constraints on the geometry such as the gas flow path, particle impact characteristics, engine mass flow rate, sand particle size and/or nacelle size for reduced drag can be used as a constraint on the design resulting in a geometry that is safe from erosion. Another important and unique advantage and strength of the inverse design technique is in its multi-point design capability (Ref. 15–18) in which multiple design requirements can be met simultaneously and, hence, the designed geometry performs equally well under "on- or off-design" conditions. The inverse design function is based on PROFOIL, the multipoint inverse airfoil design code (Ref. 16). Important details of the inversed design methodology are presented next.

The inverse airfoil design technique is based on conformal mapping of flow around a circle (known) to that around the airfoil (desired) through conformal transformation. The method was first proposed by Eppler (Ref. 15) and later extended to include multi-point design by Selig and Maughmer (Ref. 16), and further by Saeed and Selig (Ref. 17) to include design of slot-suction airfoils. The basis of the inverse airfoil design technique stems from the fact that the flow around an arbitrary airfoil may be mapped to the flow about a circle. Since the flow about the circle is easily determined, it remains only to find the transformation or the mapping. Moreover, since the mapping follows the flow or more specifically the velocity distribution, the objective in an inverse design problem is to determine the mapping from the specified airfoil velocity distribution and not from the airfoil shape. Furthermore, since the mapping derivative directly relates to the velocity distribution, it is more convenient to find the mapping derivative instead of the mapping itself. Once the mapping derivative is known, the airfoil shape is then easily determined.

Consider the flow about the unit circle centered at the origin in the ζ-plane that is mapped to the flow around an arbitrary airfoil in the z-plane via $z = z(\zeta)$ as shown in Fig. 10. The complex velocity for uniform flow of unit velocity at an angle of attack α about on the unit circle in the ζ-plane can be written as:

$$\left.\frac{dF}{d\zeta}\right|_{\zeta=e^{i\phi}} = 4\sin\left(\frac{\phi}{2}\right)\cos\left(\frac{\phi}{2}-\alpha^*(\phi)\right)e^{-i(\phi-\pi/2-\pi^*(\phi))} \quad (6)$$

where

$$\pi^*(\phi) = \begin{cases} 0, & 0 \le \phi \le \pi + 2\alpha^*(\phi) \\ \pi, & \pi + 2\alpha^*(\phi) \le \phi \le 2\pi \end{cases} \quad (7)$$

Here $\alpha^*(\phi)$ is the design angle of attack with respect to zero-lift line for a single-point design. Since the velocity distribution corresponds to the lift coefficient which in turn depends on the angle of attack, the velocity distribution along different airfoil segments can be related to different angle of attack conditions, i.e., $\alpha^*(\phi)$. The resulting airfoil will, therefore, exhibit the design characteristics, i.e. the velocity distribution $v^*(\phi)$ when operated at the corresponding $\alpha^*(\phi)$. Let the complex velocity on the surface of an arbitrary airfoil in the z-plane be:

$$\left.\frac{dF}{dz}\right|_z = v^*(\phi)e^{-i\theta^*(\phi)} \quad (8)$$

Published By:
Blue Eyes Intelligence Engineering
and Sciences Publication (BEIESP)

where $v^*(\phi)$ and $\theta^*(\phi)$ are the desired velocity and surface slope distributions, respectively. The complex velocity in the z-plane can then be mapped to the complex velocity in the ς-plane via the transformation:

$$\left.\frac{dF}{dz}\right|_z = \left(\frac{dF}{d\varsigma}\right)_{\varsigma=e^{i\phi}} \left(\frac{d\varsigma}{dz}\right)_{\varsigma=e^{i\phi}} \tag{9}$$

where the derivative of the mapping function on the unit circle is assumed to be of the form

$$\left(\frac{dz}{d\varsigma}\right)_{\varsigma=e^{i\phi}} = (a_m + ib_m)e^{1-\varepsilon}\, e^{P(\phi)+iQ(\phi)} \tag{10}$$

which must satisfy three conditions: the airfoil trailing-edge angle must be finite, the flow at infinity must be unaltered, and the airfoil contour must close. These conditions on the mapping lead to the integral constraints (Ref. 15, 16) that must be satisfied for to yield an airfoil with a finite trailing edge angle ε. To relate $v^*(\phi)$ and $\theta^*(\phi)$ to the series coefficient of the mapping derivative, substitute Eqs. (6), (8) and (9) into Eq. (10) and taking the natural logarithm of the resulting equation yields the following results

$$P(\phi) = -\ln\left\{\frac{(2\sin\phi/2)^{-\varepsilon} v^*(\phi)}{2\left|\cos(\phi/2-\alpha^*(\phi))\right|}\right\};\quad Q(\phi) = \theta^*(\phi) + \pi^*(\phi) + \varepsilon(\pi/2 - \phi/2) \tag{11}$$

where $0 \le \phi \le 2\pi$. Thus, the specification of velocity $v^*(\phi)$ and the angle of attack $\alpha^*(\phi)$ uniquely determines $P(\phi)$. Alternatively, specifying the airfoil flow direction $\theta^*(\phi)$ and $\pi^*(\phi)$, uniquely determines $Q(\phi)$. Since $P(\phi)$ and $Q(\phi)$ are conjugate harmonic functions, then from either one the corresponding harmonic function is determined through the Poisson's integral formula exterior to the circle. Once $P(\phi)$ and $Q(\phi)$ are known, the airfoil coordinates $x(\phi)$ and $y(\phi)$ are then obtained through quadrature.

The function $P(\phi)$ depends only on ϕ and is defined by specifying velocity distribution $v^*(\phi)$ and the angle of attack distribution $\alpha^*(\phi)$, termed as the design velocity and the corresponding design angle of attack distributions, respectively. Since it is only necessary that $P(\phi)$ be continuous, a discontinuity in any one or a combination of the design variables, i.e., $v^*(\phi)$ and $\alpha^*(\phi)$, must be compensated by a corresponding discontinuity in any one or a combination of the remaining design variables. This is the most important point of the theory, and it is on this basis that the multipoint design is accomplished. Thus, the airfoil can be divided into a number of segments along which the design velocity distribution along with the design values for $\alpha^*(\phi)$ are specified. It is helpful for design purposes to let $\alpha^*(\phi)$ be constant over any given segment; whereas, $v^*(\phi)$ should be allowed to vary in order to obtain some desired velocity distribution. Then, in order to ensure continuity between segments, the following condition must be satisfied.

$$P_+(\phi_i) = P_-(\phi_i) \tag{12}$$

or from Eq. (11),

$$\frac{v_-^*(\phi_i)}{\left|\cos(\phi_i/2-\alpha_-^*(\phi_i))\right|} = \frac{v_+^*(\phi_i)}{\left|\cos(\phi_i/2-\alpha_+^*(\phi_i))\right|} \tag{13}$$

where ϕ_i is the arc limit between segments i and $i+1$. For a four-segment airfoil, shown in Fig. 11, Eq. (13) will result into three relations that are commonly referred to as continuity constraints. The continuity constraints must be satisfied at the junction of the segments except at the trailing edge. Thus, different design parameters [e.g., angle of attack distribution $\alpha^*(\phi)$] may be specified with respect to different segments on the circle yielding a multipoint design. Typically, good performance is required over a range of angles of attack. For example, high-lift (high angle of attack) performance may be required as well as low-lift (low angle of attack). Thus, for instance, upper surface velocity distribution can be prescribed for a high angle of attack while simultaneously lower surface velocity distribution can be prescribed for a low angle of attack. This multi-point inverse design process is illustrated in Fig. 11 where A, B and C correspond to multiple design requirements based on, for example, the different flight segments of an aircraft.

As mentioned earlier, the specification of the velocity is not completely arbitrary and must satisfy certain integral constraints that arise due to the conditions on the mapping. These constraints come from the requirement on the mapping that the airfoil trailing edge must be closed and the velocity in the far-field must approach the free stream value. These conditions are commonly referred to as integral constraints and are mathematically expressed as:

$$\oint_{C_z} dz = \oint_{C_\varsigma} \frac{dz}{d\varsigma}d\varsigma = 0;\ \lim_{\varsigma\to\infty}\frac{dz}{d\varsigma} = 1 \tag{14}$$

where C_z and C_ς are contours about the airfoil and circle, respectively. Thus, application of the constraints to Eq. (10) suggests that the integral constrains are satisfied if and only if

$$\begin{aligned} a_0 &= \frac{1}{2\pi}\int_0^{2\pi} P(\phi)d\phi = 0 \\ a_1 &= \frac{1}{\pi}\int_0^{2\pi} P(\phi)\cos\phi d\phi = 1-\varepsilon \\ b_1 &= \frac{1}{\pi}\int_0^{2\pi} P(\phi)\sin\phi d\phi = 0 \end{aligned} \tag{15}$$

The satisfaction of these constraint leads to a system of (N+3) equations where N is the number of segments. As mentioned earlier, the specification of the velocity distributions is not completely arbitrary. It must contain an equal number of unknowns (N+3) to obtain a solution of the problem. Typically these unknowns are the velocity levels on (N-1) segments, and the remaining 4 variables define the form of the recovery and closure functions for flow at the trailing edge along the upper and lower surfaces. Additional constraints (dependent variables) such as pitching moment, maximum thickness, camber, etc., can also be imposed and satisfied through an iterative procedure by varying some independent variables in the design. Simultaneous solution of the constraints requires a multi-dimensional Newton iteration scheme and is accomplished within 10-15 iterations. Details of the mathematical formulation and various applications of the method are described in (Ref. 15-17). The final solution yields the airfoil geometry which is then used to determine flow field and the resulting sand particle impingement characteristics.

D. The Optimization Function

To carry out the optimization of the IPS system, an appropriate objective function must be defined along with the constraints.

Published By:
Blue Eyes Intelligence Engineering
and Sciences Publication (BEIESP)

The objective function chosen in this study is the engine inlet mass flow rate. The constraints could be in the form of desired operational conditions, geometric shape or size, scavenge efficiency, etc. Hence, the optimization problem at hand could involve a vast number of variables that all need to be linked to the objective function and simultaneously accounted for. To accomplish this task, a multi-variable optimization scheme is adopted. The airfoil positioning (translation, orientation and scaling) and airfoil shape parameters (airfoil camber, thickness, and/or airfoil pitching moment) are communicated by the analysis function to the optimization function to evaluate the objective function. A new IPS geometry is obtained after each design iteration. To optimize the IPS design for given operational conditions and a given engine requirement mass flow rate, the output of the objective function must be minimized to zero.

Since the objective function is non-linear and non-continuous and contains non-linear constraints, the design space needs to be searched in a random manner so that it would not get locked to a local minimum. Such traits are found in heuristic or constrained direct search methods (Ref. 39) since these methods do not require any information about the gradient of the objective function. In MATLAB, the direct search method is implemented in a generalized pattern search algorithm or function in conjunction with the Genetic Algorithm toolbox (Ref. 40). This method or function is known as Pattern Search function and was chosen to optimize the IPS design. The optimizer requires an initial guess (initial design) which is close to or inside the feasible region so that it would converge and would not get locked into a local minimum. To solve this problem, an additional program function is used which gives the designer the ability to optimize only for the inlet mass flow rate required. Use of this function has been found to yield a good initial design. The function moves elements 2 and 3 in the y-direction, changing the inlet area, and analyzes the IPS for the inlet mass flow rate and results in a design with an inlet mass flow rate very close to the design requirement

III. Results And Discussion

This section presents some of the results on both analysis and design of IPS system. The analysis examples are shown first followed by a few design examples. The examples were performed on a computer with a 3 gigahertz Intel Core 2 Extreme 6800, with a 2 gigabyte 800 MHz ram. In all the problems, the angle of attack was kept at 0 deg and the free stream velocity was set to 40 m/s. The type of sand particles was set either to very fine or medium.

A. Airfoil design example

Consider the mapping shown in Fig. 12 where a circle is divided into five segments and mapped to a five-segment airfoil. The three integral constraints on the mapping Eq. (42) require that three free parameters must be introduced to satisfy these constraints. These free parameters arise from the form of pressure recovery function used in the analysis. In addition, to satisfy the four continuity constraints Eq. (40) at the junction of the segments (s_1 through s_4 in Fig. 15), another five free parameter must be introduced to obtain a solution. These five parameters are the velocity levels at the junctions based on the desired velocity distribution $v^*(\phi)$ along each segment. Typically, only the first velocity level is specified and the rest are obtained from the four continuity constraints. Practically any desired airfoil property such as camber, thickness and pitching moment coefficient can be incorporated into the inverse design system with iteration on some inverse design parameter. For example, the pitching moment at a given angle of attack may be specified by adjusting the first velocity level. Here the airfoil shape is adjusted until the desired analysis property is obtained.

B. IPS Analysis & Design Example

Figure 13 shows results of analysis in which medium sand particles were allowed to impact and rebound after impact. As evident from the figure, the rebounding particle may easily find their way into the core flow of the engine and hence consideration of rebound characteristics is important for both analysis and design of IPS system. The new analysis routine has also been improved to consider only those particles that enter the engine between elements #1 and #4 or #5.

IV. Conclusion

Several important conclusions can be drawn from the present investigation. A new and versatile method for the design of an IPS system is now available. Details of development of the efficient design method for aircraft engine sand separator systems are presented along with the methodology used to achieve practical designs of an IPS system. The design method makes use of state-of-the-art and practical design and analysis techniques, such as the inverse aerodynamic design methodology that also takes into account viscous effects to aid in the design of specific profile shapes for engine air intakes. The sand separator design is achieved by giving a specific contour to the intake profile (such as a highly curved bend in the duct) that the contaminants because of their inertial momentum are forced away from the central flow. Since the sand particles can rebound of the air intake walls and enter the engine, the method takes into account sand particle rebound or restitution characteristics in the design. The overall design is accomplished with the aid of optimization techniques in both the inverse aerodynamic design as well as in the sand separator system design. In addition, to facilitate the design, several numerical programs and graphical user interface have been developed to aid in the design and analysis of aircraft engine sand separator systems in an interactive manner. The method has the capability to: 1) Design individual airfoil elements, 2) Orient and arrange airfoils to form a multi-element airfoil based IPS system by employing translational, scaling and rotational functions, 3) Carryout 2D flow and trajectory analysis of multi-element airfoil based IPS system including impact and rebound off surfaces, and 4) perform design optimization using pattern search – a genetic algorithm based optimization technique. The study paves way for incorporating erosion in the design in a follow-up project.

Published By:
Blue Eyes Intelligence Engineering
and Sciences Publication (BEIESP)

V. Acknowledgment

The author acknowledges the support provided by King Abdulaziz City for Science and Technology (KACST) through the National Science & Technology Unit at King Fahd University of Petroleum & Minerals (KFUPM) for funding this work under project # 08-SPA49-4 as part of the National Science, Technology and Innovation Plan.

References

1. Tabakoff, W., and Hamed, A., “Installed Engine Performance in Dust Laden Atmosphere,” AIAA Paper 1984-2488, 1984.
2. van der Walt, J. P., and Nurick, A., “Prediction of Helicopter Engines Fitted with Dust Filters,” *AIAA Journal of Aircraft*, Vol. 23, No. 1, Jan.—Feb. 1995, pp.118-123.
3. Mann, D., “Case Studies in TRIZ: Helicopter Engine Particle Separator,” *The TRIZ Journal* [online], Feb. 1999, http://www.triz-journal.com/archives/1999/02/a/index.htm (retrieved 10 April 2010).
4. J. Tariq, “Operating Aircraft in Gulf Environment,” presented at the Regional Aviation Symposium organized by Saudi Aramco Aviation, Nov. 6, 2007.
5. Hamed, A., Tabakoff, W., and Wenglarz, R., **“**Erosion and Deposition in Turbomachinery,” *AIAA Journal of Propulsion and Power*, Vol. 22, No. 2, March–April 2006.
6. Tabakoff, W., and Simpson, G., “Experimental Study of Deterioration and Retention on Coated and Uncoated Compressor and Turbine Blades,” AIAA Paper 2002-2373, Jan. 2002
7. Abedi, M., “Effect of Restitution Coefficient on Inertial Particle Separator’s efficiency,” *Mechanical Engineering Master's Theses, Northeastern University,* Paper 17, 2009. http://hdl.handle.net/2047/d1001925x (retrieved 10 April 2010).
8. Vittal, B. V. R., Tipton, D. L., and Bennett, W. A., “Development of an Advanced Vaneless Inlet Particle Separator for Helicopter Engines,” *AIAA Journal of Propulsion and Power*, Vol. 2, No. 5, 1986, pp. 438-444.
9. Breitman, D. S., Dueck, E. G., and Habashi, W. G., “Analysis of a Split-Flow Inertial Particle Separator by Finite Elements,” *AIAA Journal of Aircraft*, Vol. 22, No. 2, 1985, pp. 135-140.
10. Zedan, M., Mostafa, A., Hartman, P., and Sehra, A., “Viscous Flow Analysis of Advanced Particle Separators,” *AIAA Journal of Propulsion and Power*, Vol. 8, No. 4, 1992, pp. 843-848.
11. Saeed, F., and Al-Garni, A. Z., “System for Inertial Particles Separartion,” US Patent No. 7922784, issued by the US Patent & Trademark Office on April 12, 2011.
12. Saeed, F., Al-Garni, A. Z., “Analysis Method for Inertial Particle Separator,” *AIAA Journal of Aircraft*, Vol. 44, No. 4, Jul.–Aug. 2007, pp. 1150-1158.
13. Al-Faris, E., and Saeed, F., “Design and Optimization Method for Inertial Particle Separator Systems,” *AIAA Journal of Aircraft*, Vol. 46, No. 6, Nov.-Dec. 2009, pp. 1919-1929.
14. Dai, L., Yu, M., and Dai, Y., “Nozzle Passage Aerodynamic Design to Reduce Solid Particle Erosion of a Supercritical Steam Turbine Control Stage,” *Wear*, Vol. 262, 2007, p. 104–111.
15. Eppler, R., *Airfoil Design and Data*, Springer – Verlag, New York, 1990.
16. Selig, M. S., and Maughmer, M., “Multipoint Inverse Airfoil Design Method Based on Conformal Mapping,” *AIAA Journal*, Vol. 30, No. 5, May 1992, pp. 1162-1170.
17. Saeed, F., and Selig, M. S., “A Multipoint Inverse Airfoil Design Method for Slot-Suction Airfoils,” *AIAA Journal of Aircraft*, Vol. 33, No. 5, Jul.–Aug. 1996, pp. 708-715.
18. Selig, Michael S., “PROFOIL – A Multipoint Inverse Airfoil Design Method, User’s Guide”, Cleveland Ohio, Feb. 1999.
19. Tuncer, C., *An Engineering Approach to the Calculation of Aerodynamic Flows*, Horizon Publishing Inc. (Springer), California, 1999.
20. Saeed, F., Brette, C., Fregeau, M., Trifu, O., and Paraschivoiu, I., “A Three-Dimensional Water Droplet Trajectory and Impingement Analysis Program,” AIAA Paper 2005-4838, June 2005.
21. Saeed, F., “State-of-the-Art Aircraft Icing and Anti-Icing Simulation,” *ARA (American Romanian Academy) Journal*, Vol. 2000-2002, No. 25-27, June 2002, pp. 106-113.
22. Langmuir, I., and Blodgett, K. B., “A Mathmatical Investigation of Water Droplet Trajectories,” US Army Air Forces TR 5418, Feb. 1946 (Contract No. W-33-038-ac-9151 with General Electric Co.). Also US Department of Commerce Publication Board (PB) No. 27565.
23. Bragg, M. B., “A Similarity Analysis of the Droplet Trajectory Equation,” *AIAA Journal*, Vol. 20, No. 12, Dec. 1982, pp. 1681-1686.
24. Fehlberg, E., “Classical Eighth- and Lower-Order Runge-Kutta-Nyström Formulas with a New Stepsize Control Procedure for Special Second-Order Differential Equations,” NASA Technical Report R-381, March 1972.
25. Chhabra, R. P., Agarwal, L., and Sinha, N. K., “Drag on Non-Spherical Particles: An Evaluation of Available Methods,” *Powder Technology*, Vol. 101, No. 3, March 1999, pp. 288—295.
26. Taslim, M. E., Khanicheh, A., and Spring, S., “A Numerical Study of Sand Separation Applicable to Inlet Particle Separator Systems,” *Journal of the American Helicopter Society*, Vol. 54, No. 042001, 2009.
27. Taslim, M. E., and Spring, S., “A Numerical Study of Sand Particle Distribution, Density, and Shape Effects on the Scavenge Efficiency of Engine Inlet Particle Separator Systems,” *Journal of the American Helicopter Society*, Vol. 55, No. 022006, 2010.
28. Laitone, J. A., “Characterization of Particle Rebound Phenomena in the Erosion of Turbomachinery,” *AIAA Journal of Aircraft*, Vol. 20, No. 3, March 1983, pp. 275-281.
29. Tabakoff, W., and Hamed, A., “Installed Engine Performance in Dust-Laden Atmosphere,” AIAA Paper 84-2488, AISS/AHS/ASEE Aircraft Design Systems and Operations Meeting, San Diego, CA, Oct. 21–Nov. 2, 1984.
30. Gunn, R., and Kinzer, G. D., “The Terminal Velocity of the Fall of Water Droplets in Stagnant Air,” *J. Meteor.*, 6, 243-248, 1949.
31. Chen, X., McLaury, B. S., and Shirazi, S. A., “Application and Experimental Validation of a Computational Fluid Dynamics (CFD)-Based Erosion Prediction Model in Elbows and Plugged Tees,” *Computers & Fluids*, Vol. 33, 2004, pp. 1251–1272.
32. Fair, G., and Geyer, J., *Water Supply and Waste Water Disposal*, John Wiley, New York, 1954.
33. Clift, R., Grace, J. R., and Weber, M. E., *Bubbles, Drops, and Particles*, Academic Press, New York, 1978.
34. Flemmer, R. L. C., and Banks, C. L. “On the Drag Coefficient of a Sphere,” *Powder Technology*, Vol. 48, No. 3, 1986, pp. 217–221.
35. Haider, A., and Levenspiel, O., “Drag Coefficient and Terminal Velocity of Spherical and Nonspherical Particles.’’ *Powder Technology*, Vol. 58, 1989, pp. 63–70.
36. Turton, R., and Levenspiel, O., “A Short Note on the Drag Correlation for Spheres,” *Powder Technology*, Vol. 47, 1986, pp. 83–86.
37. Khan, A. R., and Richardson, J. F., “The Resistance to Motion of a Solid Sphere in a Fluid,” *Chem. Eng. Commun*.,Vol. 62, 1987, pp. 135–150.
38. Brown, P. P., and Lawler, D. F., “Sphere Drag and Settling Velocity Revisited,” *Journal of Environmental Engineering*, Vol. 129, No. 3, March 2003, pp. 222-231.
39. Reklaitis, G. V., Ravindran, A., and Ragsdell, K. M., *Engineering Optimization: Methods and Applications*, Wiley-Interscience, 1983.
40. MATLAB 7.0, The MathWorks, Inc., Natick, MA, 2008 http://www.mathworks.com/ (retrieved 10 April 2010).

(a) High pressure turbine vanes

Published By:
Blue Eyes Intelligence Engineering
and Sciences Publication (BEIESP)

(b) High pressure turbine blades

Fig. 1. Effects of sand erosion on high pressure turbine (a) vanes and (b) blades of aircraft engines operating in the Saudi Arabian desert environment. (Courtesy: Tariq Jabr, Saudi Aramco Aviation)

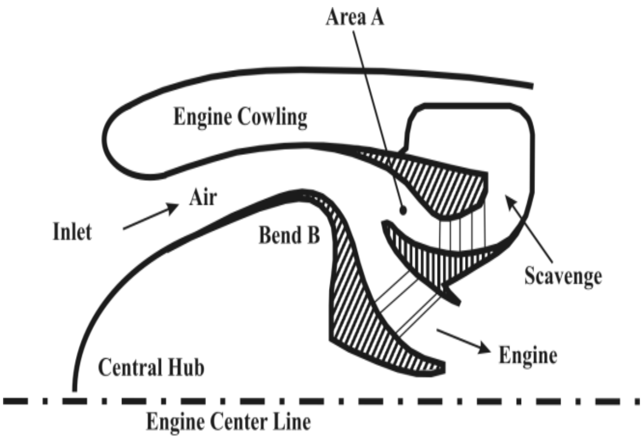

Fig. 2. Typical axisymmetric helicopter engine particle separator (Adapted from Ref. 3)

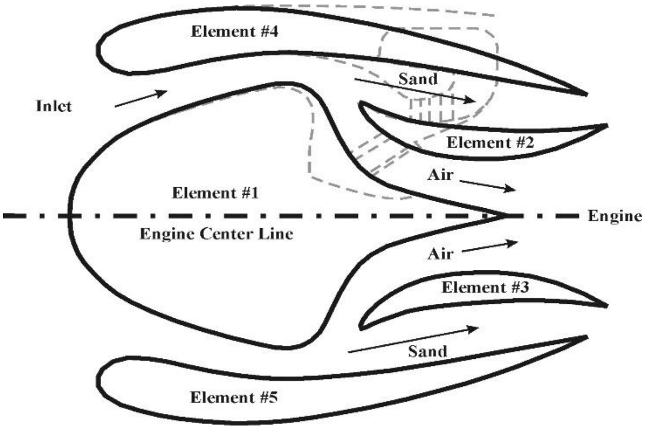

Fig. 3. A five-element airfoil configuration model for IPS system

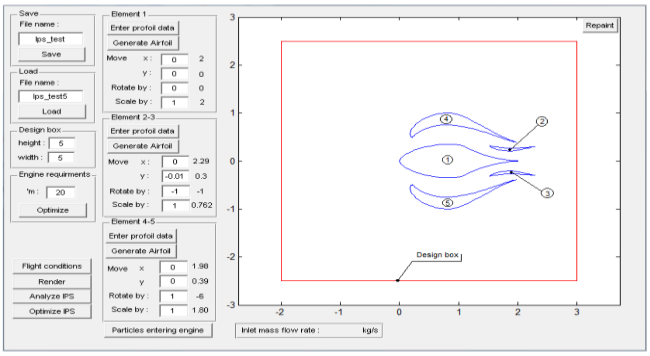

Fig. 4. The MATLAB GUI for IPS system analysis and design

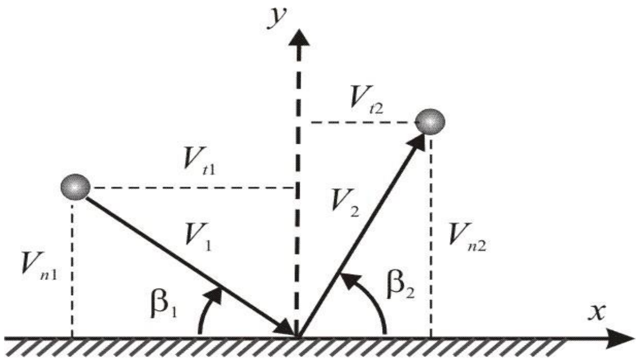

Fig. 5. Sand particle impact and rebound characteristics

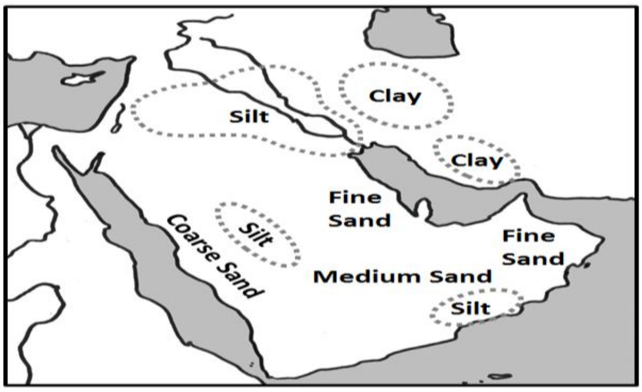

Fig. 6. Map of soil grain sizes in the Middle East. Courtesy of National Center for Atmospheric Research (NCAR). (Adapted from Ref. 7)

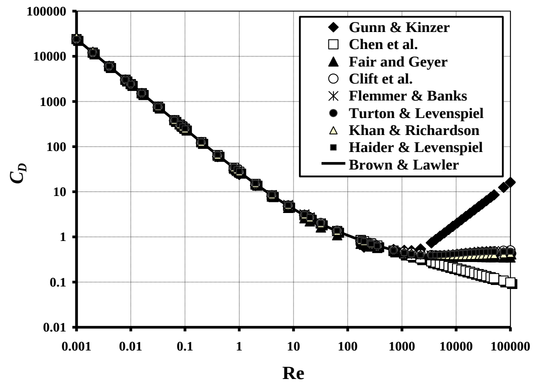

Fig. 7. Comparison of sphere drag correlations by various authors

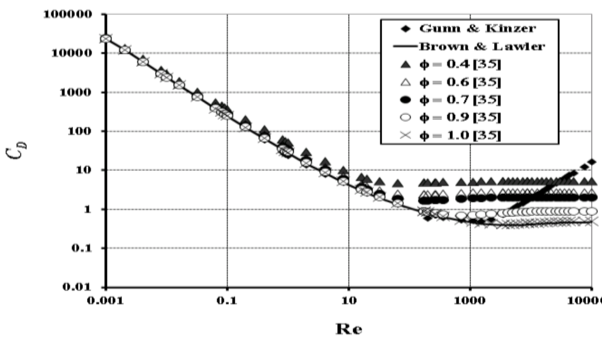

Fig. 8. Comparison of non-spherical and spherical particle drag correlations by various authors

Published By:
Blue Eyes Intelligence Engineering and Sciences Publication (BEIESP)

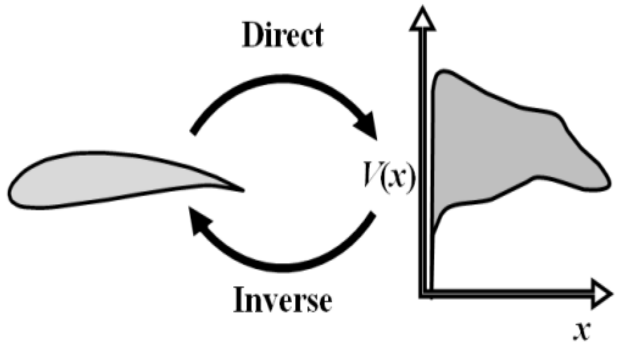

Fig. 9. Direct vs. inverse approach to airfoil design

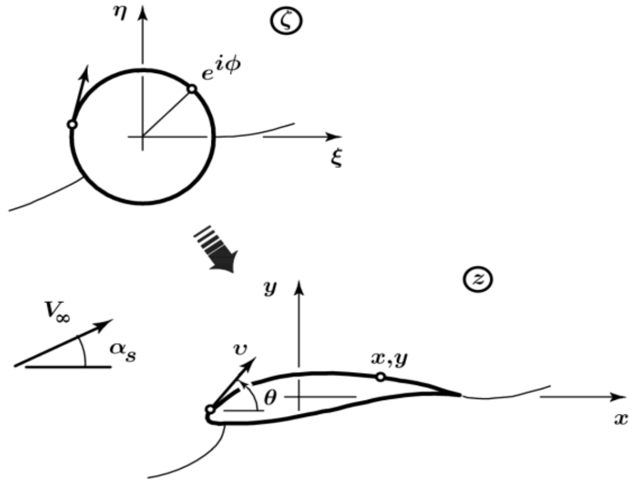

Fig. 10. Mapping from circle to airfoil plane

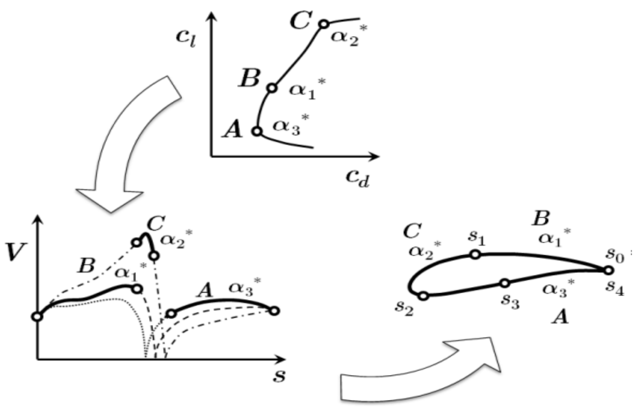

Fig. 11. The multi-point inverse airfoil design process

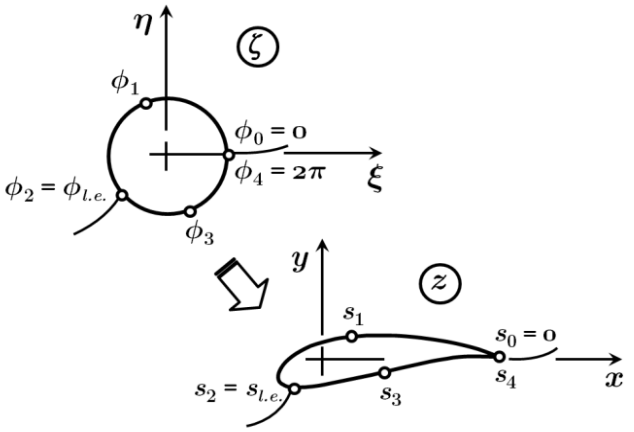

Fig. 12. Circle divided into four segments and mapped to a four-segment airfoil

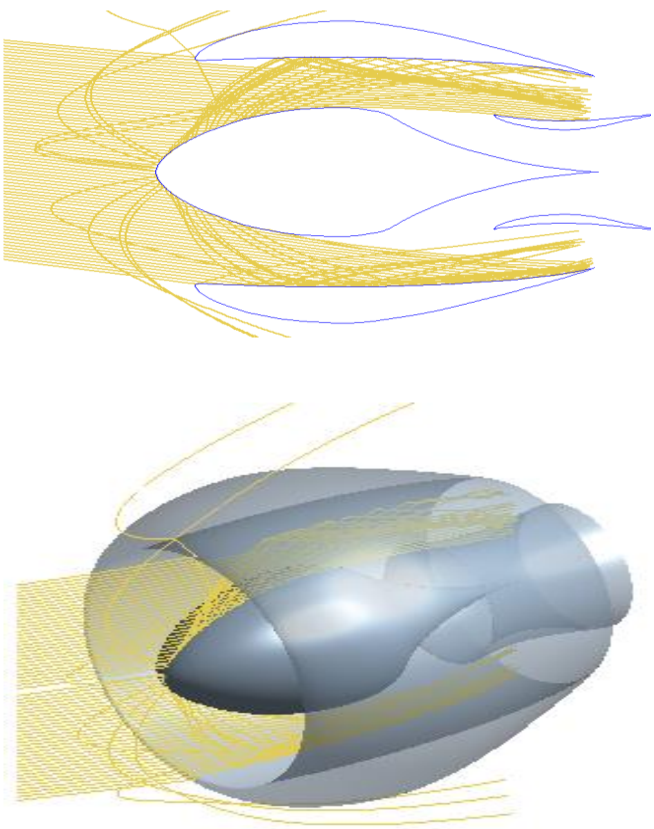

Fig. 13. IPS design example and its 3D rendering

Dr. Farooq Saeed, is a graduate of the University of Illinois at Urbana-Champaign where he earned both his Master's and Doctorate degree in Aeronautical & Astronautical Engineering. Dr. Farooq is also certified in aircraft maintenance and has served as maintenance officer, supervisor and instructor in the Pakistan Army Aviation. Dr. Farooq is also a FAA certified private pilot with instrument rating as well as has completed requirements for commercial pilot license. Dr. Farooq has a very strong interest in Aviation Science and Aerospace Engineering related fields. He is also very active in research and has collaborated with NASA, Boeing, Bombardier Aerospace, MIT, NSERC, KACST and several other organizations. His research interests include airfoil design for various applications including VAWTs, experimental and numerical aerodynamics, CFD, wind energy system design, aircraft design, anti-icing system analysis & design, sand particle separator system design, etc., to name a few.

Published By:
Blue Eyes Intelligence Engineering
and Sciences Publication (BEIESP)